



An electrically switchable dye-doped liquid crystal polarizer for organic light emitting-diode displays

Yuri Won^a, Hoon Sub Shin^{a,b}, Mira Jo^a, Young Jin Lim^a, Ramesh Manda^{a,*}, Seung Hee Lee^{a,*}

^a Department of Nanoconvergence Engineering and Department of Polymer Nanoscience and Technology, Jeonbuk National University, Jeonju, Jeonbuk 54896, Republic of Korea

^b LG Display Co., Ltd., Gumi, Gyungbuk 39405, Republic of Korea

ARTICLE INFO

Article history:

Received 3 December 2020

Received in revised form 5 February 2021

Accepted 13 March 2021

Available online 16 March 2021

Keywords:

Organic light-emitting diode

Dichroic dye

Switchable polarizer

Dye-doped liquid crystal

ABSTRACT

A conventional polarizer for an organic light-emitting diode (OLED) display deteriorates light efficiency by blocking more than 50% of the emitted light from the OLED. The use of such a polarizer with a quarter-waveplate is inevitable to achieve an excellent dark state because it blocks the reflection of incoming ambient light to the OLED. However, when there is no incoming light outside of the display, the polarizer does not play a role of suppressing the reflection but sacrifices emitted light. In this study, we propose a switchable dye-doped liquid crystal (DDL) that serves as a polarizer for strong ambient light in the voltage-off state, which effectively absorbs ambient light reflection from OLED electrodes. With the DDL in the voltage-on state, it can be switched to a non-absorption state for weak ambient light, allowing the emitted light from the OLED to pass through it, which enhances the light efficiency of the OLED. Consequently, the switchable DDL performs effectively in terms of display contrast ratio and light efficiency for any ambient light conditions. The 2 wt% DDL polarizer not only exhibits a smaller reflectance than that of a conventional polarizer, but also improves the emission intensity by 61%. Our proposed DDL polarizer can be compactly equipped with an OLED panel and can improve the lifetime of the device by enhancing optical efficiency.

© 2021 Elsevier B.V. All rights reserved.

1. Introduction

Recently, organic light-emitting diode (OLED) devices are emerging as a promising technology for smartphones and even televisions because of their self-luminous displays with high color gamut, flexibility, high contrast ratio, and wide viewing angle [1–6]. Generally, the OLED display consists of multiple organic layers confined between anode and cathode electrodes in which the organic layers inject electrons and holes into the emission layer and a recombination of electrons moving in opposite direction results in the emission of light. In the display, the cathode is typically a mirror-like metal layer that causes strong reflections of ambient light to enter into the OLED panel [7,8]. The reflection causes a serious issue of low contrast ratio display. For instance, under direct sunlight or inside a bright room the reflection can become stronger such that a good dark cannot be achieved and the contrast ratio of the displayed image becomes very poor, rendering the exhibited display with low visibility.

Several attempts to overcome this issue have been made such as developing potential alternatives to metal electrodes [9–12]; the use of antireflection coatings [13]; work with black matrix and absorption layers

[14,15]; and suggesting various types of models to enhance destructive interference in the reflection or scattering of ambient light [16–18]. The most notable and efficient commercialized method is to use a circular polarizer which combines a linear polarizer with a wide-band quarter-wave retardation plate (QWP) and can prevent ambient reflections by rotation of the polarization state of an incident light [1,19–21]. This approach provides a substantial increase in contrast ratio owing to the improved dark state in ambient light conditions; however, severe loss of emitted light by more than 50% with an OLED device is inevitable. The higher the degree of polarization (DOP) of a polarizer, the more its transmittance drops. A commercialized polarizer with DOP transmits only 44% of the emitted light. Consequently, the prospect of the indoor performance of the device on light efficiency, especially when there is no or weak light less than 200 lx, has to be forfeited [19,22,23]. The drawback of an OLED device is the relatively short lifetime of the emitted organic materials compared to the inorganic materials of LED or voltage-driven liquid crystal displays. An OLED device's lifetime gets shorter with higher electroluminescent light. In turn, if we can improve the luminance of an OLED by 50% in relatively low ambient light, then the lifetime of the OLED can be enhanced and extended. In order to overcome the above mentioned technical barriers, a polarizer needs to be developed that can switch from a linear polarizer to perfect transparency depending on intensity of ambient light. Carbon-based tunable

* Corresponding authors.

E-mail addresses: rameshmanda@jbnu.ac.kr (R. Manda), lsh1@jbnu.ac.kr (S.H. Lee).

polarizers such as carbon nanotubes and graphene oxide have been proposed, however, their DOP and large-scale optical performance are still far away from commercialization [24–27].

In this report, we propose a switchable dye doped liquid crystal (DDLC) polarizer to enhance the on-state efficiency of OLED displays. The proposed DDLC polarizer consists of homogeneously aligned dichroic black dye in a nematic LC host and can be switched between high and low absorption states. The DDLC, then, absorbs ambient light with polarization propagating parallel to the long axis of the black dye in a voltage-off state and passes through the emitted light from the OLED without absorption in the voltage-on state. Consequently, the electrically switchable DDLC polarizer not only works as a polarizer under strong ambient light conditions, but also significantly improves the optical efficiency of the display when ambient light is low. Our studies show that a DDLC polarizer with 2 wt% doped dye exhibits less specular and diffuse reflectance than that of a conventional polarizer. In addition, our polarizer shows ~61% increase in display emissions upon voltage supply, which in turn avoids the requirement of an unnecessary increase in emission power to exhibit a high luminance at low ambient light. Furthermore, the DDLC polarizer can increase lifetime of OLED owing to improvement in optical efficiency.

2. Cell structure and the driving principle of DDLC polarizer

A conventional bottom-emission OLED display device consists of a light emission unit (OLED panel), a QWP film, and a linear polarizer. The polarizer is set between the QWP and the OLED panel wherein its transmission axis is positioned 45° to the slow axis of the QWP as depicted in Fig. 1(a) and (b). The principle of suppressing a strong ambient light is to utilize a circular polarizer. When unpolarized ambient light hits the display panel, it is converted to linearly polarized light by the polarizer and then is converted to circular polarized light by QWP film. Once it is reflected from the metal electrode, the light becomes circularly polarized but with an opposite sense and then finally the linearly polarized light, after passing through the QWP in a polarization state, becomes orthogonal to the polarizer axis [28,29]. The polarizer, then, blocks the light, as shown in Fig. 1(a). The demerit of this approach is that it also blocks portions of emitted light from the OLED when the display is turned-on, resulting in a more than 50% loss of emitted light, as shown in Fig. 1(b). The underlying mechanism of our DDLC polarizer relies on the selective absorption of ambient light such that the light propagating parallel (perpendicular) to the long axis of the black dye is absorbed (transmitted). The dye aligns parallel to the LC director and when the LC is electrically switched to orient perpendicular to a substrate, the dye follows the orientation of the LC director. The higher the dichroic ratio of a black dye, the higher the transmittance in the

voltage-on state will be. Therefore, a proper concentration of black dye with an appropriate cell gap will give rise to a linearly polarized light when nonpolarized light passes through the DDLC. The proposed OLED display utilizes an electrically switchable DDLC which consists of an OLED panel, a QWP film, and a DDLC polarizer as shown in Fig. 1(c) and (d). The absorption axis of the DDLC sample is set to 45° of the slow axis of the QWP. The DDLC plays the role of a polarizer in the voltage-off state while the OLED is in emission mode, which we name the polarization mode (or P-mode), as shown in Fig. 1(c). The dye molecules are horizontally oriented in a specific direction along with the LC at which the dye molecules absorb the ambient light with a polarization state parallel to their long molecular axis while the polarization state perpendicular to the long axis of dyes passes through it. In turn, the ambient light that enters into the display panel and is converted to a linearly polarized light with a polarization axis perpendicular to the average orientation of the dye molecules in the P-mode. The reflected ambient light is effectively blocked by the DDLC polarizer, playing exactly the same role as a conventional polarizer. However, when the ambient light is not strong enough, such as inside a room with closed windows, or there is no ambient light, the DDLC device can be switched into a low absorption state, i.e. the dye molecules are aligned perpendicular to the substrate by supplying voltage to the DDLC cell. Most of the emission light passes through the DDLC polarizer without absorption by dye molecules (we call this the transmittance mode or T-mode), as shown in Fig. 1(d). Consequently, the loss of emitted light from the OLED panel will be minimized and less current can be applied to the panel to get the same luminance as the conventional approach, which can extend the lifetime of the OLED panel. The amount of light absorption that occurs in the T-mode depends on the dichroic ratio of dyes in a LC. The higher the dichroic ratio, the less absorption that occurs in the T-mode. Furthermore, when the climate affects light, such as when there is cloud cover, then an intermediate stage for the DDLC polarizer, one between homogeneously aligned and vertically aligned states, could be utilized by supplying intermediate voltage. In this way, the polarization ratio of the DDLC polarizer decreases but blocks the amount of light still coming through despite weather conditions and improves transmittance compared to conventional static polarizer. The proposed approach can improve an optical efficiency of OLED television and extend the lifetime of the OLED. In addition, rapid switching between the P- and T-modes takes place within a tenth millisecond and the DDLC exhibits excellent reliability because the voltage driven LC-dye system demonstrates a very reliable electro-optic performance [30,31]. Overall, we can effectively control the unwanted reflection of ambient light and get the desired emission intensity from an OLED panel to realize a high contrast ratio in any amount of ambient light and a long display life that covers the weak points in an OLED's lifespan.

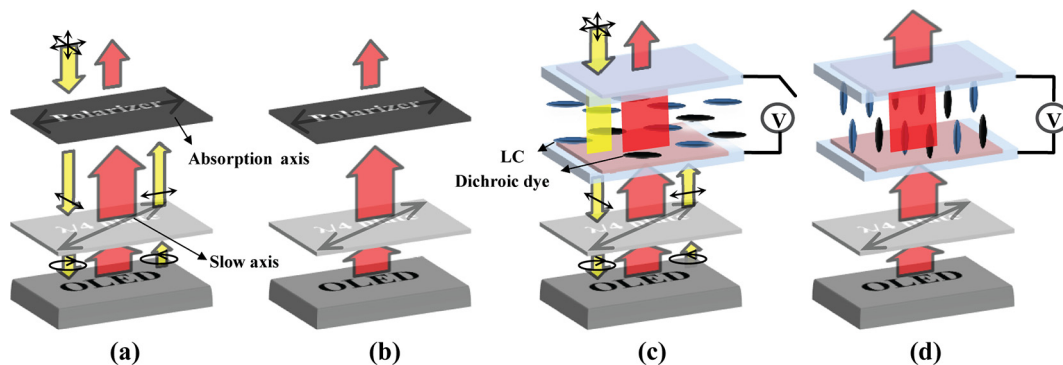


Fig. 1. Schematic representation of the working principle of the conventional circular polarizer in OLED: (a) An ambient light changes to a linearly and circularly polarized light after passing through a polarizer and QWP plate and then it changes polarization direction by 90° after reflection so that the ambient light can be blocked; (b) Light emitted by the OLED is lost by a polarizer by more than 44%. The switching principle of the DDLC polarizer in the OLED: (c) P-mode for high ambient light (DDLC plays the role of the linear polarizer); and (d) T-mode for no ambient light (DDLC transmits most of emitted light). The yellow arrows indicate an ambient light propagating into the OLED panel. The green arrows indicate an emitted light from OLED panel. The red arrows represent the polarization state of an ambient light.

3. Experiments

The DDLC polarizer proposed in this report is composed of a dichroic dye Irgaphor Black X12 (BASF Co., Korea) dispersed in a nematic LC (Merck Co., Korea). The LC exhibits a positive dielectric anisotropy of 4.7. The employed black dye exhibits a positive dichroism. The OLED panel was used as a display source. First, 1 wt%, 1.5 wt%, and 2 wt% of dichroic dye were added to the LC and mixed thoroughly by magnetic stirring for 10 min to achieve a homogeneous mixture. The mixture was then poured into the experimental cell at slightly above the T_{NI} of the LC by a capillary action. Although the dye is not known to have the tendency of forming agglomerations in the LC medium [32], in practice we have observed agglomerations for higher dye concentrations of 5 wt% that severely affects device performance. For this reason, our analysis was constrained to 2 wt% dye concentration. The experimental cell was fabricated by assembling two indium-tin-oxide glass substrates whose inner surfaces were coated with polyimide for a homogeneously planar orientation of the LC molecules, and this is schematically illustrated in Fig. S1. Both substrates were coated with polyimide (AL22620, JSR Corp.) and performed pre-baking at 80 °C for 5 min followed by a post-baking at 230 °C for 60 min. Next, both substrates were rubbed with velvet cloth and assembled antiparallel to the rubbing directions. A 5 μm cell gap tape was used to maintain the uniform gap between the substrates. Our results are quantitatively compared with the conventional film-type polarizer purchased from Dongwoo Fine-Chem Co., Korea.

We start our analysis by performing essential characterizations of the DDLC polarizer using a polarizing optical microscope (POM) (Nikon, ECLIPSE E600, Japan) attached with camera (Nikon, DXM 1200) and an optical microscope (OM). Note that only a single polarizer was used for the OM, whereas crossed polarizers were used for the POM. Next, our analysis was extended to examining reflection properties by integrating our DDLC polarizer into the OLED panel. The reflection properties were estimated by measuring luminance with two different approaches: the luminance meter method and the integrating sphere method. In first method, the reflectance measurements were performed using a luminance measurement system (ARSN-733, JASCO). With the second method, the reflectance was evaluated by an integrated sphere method that uses a spectrophotometer (CM-2600d, Konica Minolta Sensing Korea Co.). Both instruments consist of inbuilt light sources and measured the specular component included (SCI) and specular component excluded (SCE) reflections. To appraise the reflectance under day light illuminant conditions, the chromaticity behavior of the device was estimated by measuring color coordinates using the International Commission on Illumination (CIE) standard charts with Standard Illuminant D65. For wavelength-dependent transmittance measurements, a UV-Vis/NIR spectrometer (V-670, JASCO) was used and a film-type polarizer (Dongwoo Fine-Chem Co., Korea) was fixed appropriately when required. An incident of unpolarized light is converted into linearly polarized light using a film-type polarizer and detected with a transmitted light. The voltage-dependent measurements were performed by LCMS-200 (Sesim Photonics Technology, Korea) at a 60 Hz frequency. A QWP film was attached to the DDLC polarizer at which the rubbing direction makes 45° to the QWP and the images were taken in a direction normal to the substrate.

4. Results and discussion

Our analysis begins with the essential characterization of the DDLC polarizer by investigating the absorption spectra of the dye, thereby calculating dichroic ratio, order parameters, and dichroism. The absorption parallel (A_{\parallel}) and perpendicular (A_{\perp}) direction to the rubbing direction (D) was measured by polarized UV-Visible spectra. In other words, the A_{\parallel} and A_{\perp} refers to the light absorption parallel and perpendicular to average orientation of the dye, respectively. It is worth noting that the A_{\parallel} was relatively higher than the A_{\perp} , as shown in Fig. 2(a). Since,

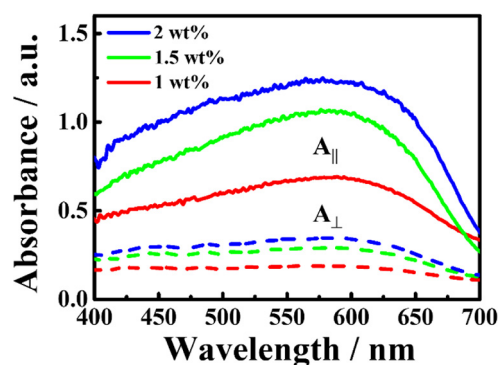


Fig. 2. Absorption spectra of DDLC polarizers with a different weight percent of dye into the LC mixture. Solid lines correspond to A_{\parallel} and dashed lines correspond to A_{\perp} .

the LC molecules are known to the non-absorption material through visible light, this polarization selective absorption is purely attributed to the dichroic dye. It is evident that the employed dye material was exhibiting a broad absorption peak covering the entire visible wavelength range. A positive dichroism was observed and a significant change of absorbance with concentrations was noticed. The dichroic ratio, which is defined as $\frac{A_{\parallel}}{A_{\perp}}$, was calculated as 3.59, 3.58 and 3.61 for 1 wt%, 1.5 wt%, and 2 wt% dye samples at 550 nm, respectively. Regardless of dye concentrations, the dichroic ratio was found to be constant for all the samples. Based on this, we further estimated the degree of orientation of dye molecules in the LC medium by measuring the order parameter (S) defined as [33],

$$S = \frac{A_{\parallel} - A_{\perp}}{A_{\parallel} + 2A_{\perp}} \quad (1)$$

where the S varies from zero (for a highly disordered system) to 1 (for a highly ordered system). The measured S does not seem to change with dye concentration. Specifically, it was found to be approximately 0.46 for all the samples measured at 550 nm. It is noteworthy to mention that the calculated order parameter data has a good correlation with obtained experimental data.

Next, we carried out our investigation to assess the voltage-dependent orientation of the dye molecules in a host LC. The optical images and corresponding voltage-dependent absorption spectra were measured to estimate the degree orientation of dye. In Fig. 3(a), the dark state under crossed polarizers changed to a bright state on 45° rotation of sample which suggests the LC directors align along the rubbing direction, i.e., planar orientation. Additionally, the intensity in the bright state decreases with increasing dye concentration. By applying the appropriate voltage at this position, the bright state again changes to a dark state due to the reorientation of the LC molecule perpendicular to the substrate along the vertical electric field. The dye molecules are also expected to follow the LC orientation. However, the images in Fig. 3(a) does not directly show the dye orientation. In turn, we measured the voltage-dependent absorption spectra with an incident polarized light with its polarization direction fixed along the D without using an analyzer. The data shown in Fig. 3(b) clearly suggest the absorption of the incident light in the voltage-off and the voltage on states shows a clear difference, proving the orientation of dye follows field-induced reorientation of the LC director. As one can expect, the absorption intensity also tends to increase with dye concentration. This is to say, the higher the dye concentration, the higher the absorption in both voltage-off and voltage-on states. As shown in Fig. 3(c), OM characterizations were performed to get a qualitative analysis of how well the DDLC polarizer performs compared to a conventional polarizer. The DDLC polarizer with 1 wt% and 1.5 wt% showed some level of light leakage when its absorption axis was orthogonal to that of a conventional

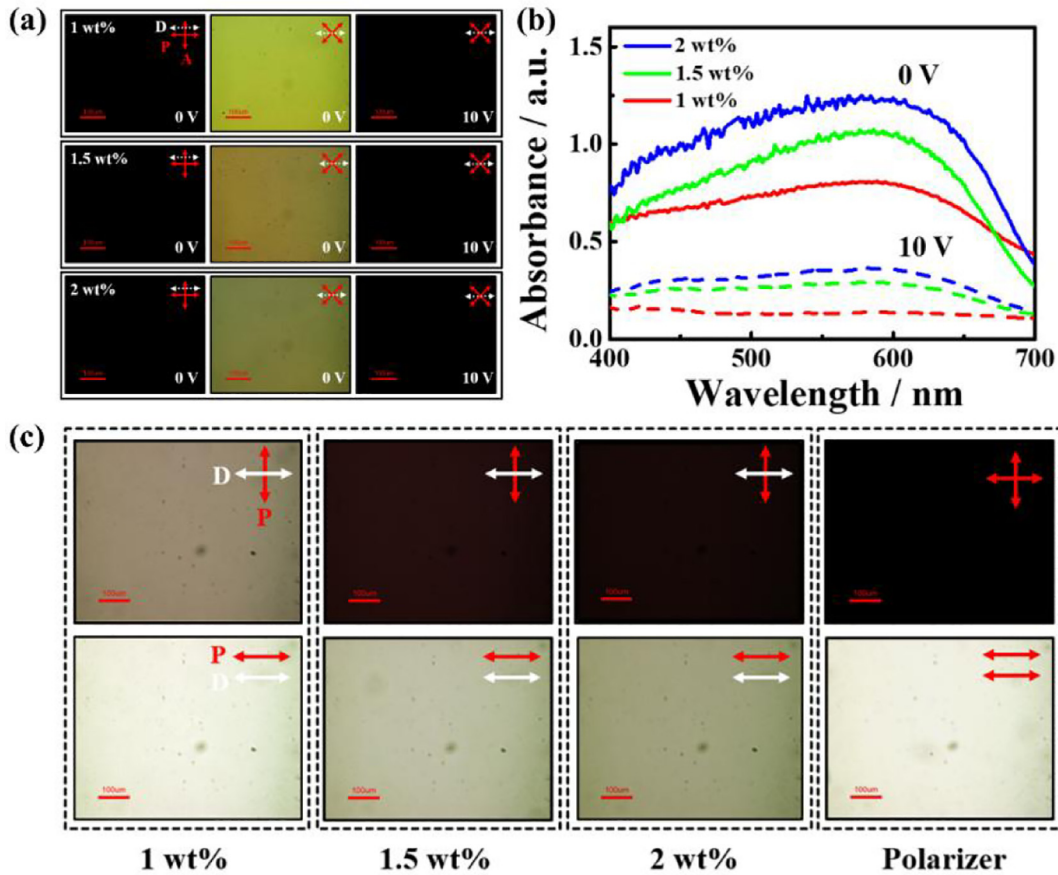


Fig. 3. (a) POM images of DDLC polarizer. *P*, *A*, and *D* represent the polarizer, analyzer, and rubbing direction of the cell, respectively. The first column represents *D* parallel to the incident polarization and the middle column refers to the rotation of the sample to 45° with respect to *P*. The last column is the sample's textures at 10 V. (b) Voltage-dependent absorption spectra of DDLC polarizers. Here, the incident light polarization state coincides with *D*. Solid and dashed lines corresponds to 0 V and 10 V, respectively. (c) OM images of DDLC polarizer with the polarization axis of an incident light perpendicular (top row) and parallel (bottom row) to the *D*.

polarizer, implying its degree of polarization was inferior to that of a conventional polarizer. However, the DDLC polarizer with 2 wt% showed a comparable dark state when its absorption axis was orthogonal to a conventional polarizer, but its transmittance became lower when it was parallel to a conventional polarizer, compared to those with conventional polarizer. In sum, the DDLC polarizer manifested polarization selective absorption and the 2 wt% doped cell showed a comparable performance in the crossed polarizer condition. The utilized dye followed the ordered orientation of the LC to effectively switch between the two distinct absorption states via bias voltage.

We extended our observations to study the wavelength-dependent transmittance of the short and long molecular axis of the dichroic dye. The transmittance parallel (perpendicular) to the transmission axis of the dye is indicated by T_{\parallel} (T_{\perp}), and the measurements scheme is shown in Fig. 4(a). Analysis of the three samples shown in Fig. 4(b) reveals that the transmittance was significantly affected by the dye concentration. The T_{\parallel} was much higher than that of the T_{\perp} for all the DDLC polarizers, indicating the emitted light from OLED panel can be greatly improved if T_{\parallel} can be switched to T_{\perp} mode. The wavelength dispersion of the DDLC polarizer was less in T_{\parallel} but stronger in T_{\perp} compared to those in conventional polarizer. The measured T_{\parallel} values are 74.4%, 64.8%, and 59.4% for 1 wt%, 1.5 wt%, and 2 wt% dye DDLC polarizers, respectively, whereas a conventional polarizer exhibits 82% transmittance. Such a significant difference between T_{\parallel} and T_{\perp} was achieved from anisotropic absorption of the dye molecules. Another interesting point to emphasize is that the T_{\perp} was also decreasing with increasing dye concentration such that the 2 wt% dye DDLC sample was exhibiting similar T_{\perp} to that of the conventional polarizer. In order to

estimate polarization ability, we measured the degree of polarization (DOP) defined as [34],

$$DOP(\%) = \sqrt{\frac{T_{\parallel} - T_{\perp}}{T_{\parallel} + T_{\perp}}} \times 100 \quad (2)$$

As displayed in Fig. 4(c), the DOP was strongly affected by the concentration of the dichroic dye and wavelength (see Fig. S2 and Fig. S3). Remarkably, the DOP of DDLC polarizers increased with dye concentration even though the T_{\parallel} decreased more with a higher dye concentration. In our measurements, the DOP of the conventional polarizer was approximately 99.7% whereas the DDLC polarizer with 1 wt%, 1.5 wt%, and 2 wt% dye concentration exhibited 89.5%, 94.2%, and 96.9% of DOP, respectively. Slightly low DOP for 1 wt% DDLC polarizer is attributed from the low absorption of the dichroic dye in T_{\perp} . Further, the Extinction Ratio (ER) of the DDLC polarizer was measured which is defined as $10 \times \log\left(\frac{T_{\parallel}}{T_{\perp}}\right)$. From Fig. 4(d), the ER is 9.4, 12.6, and 15.4 for 1 wt%, 1.5 wt%, and 2 wt% dye concentrations at 550 nm, respectively, which is smaller compared to conventional iodine-type polarizer (ER = 23.5). However, it is a high value compared to tunable polarizers reported elsewhere [35,36].

Next, we investigated a voltage-dependent transmittance of the DDLC polarizer for an unpolarized incident light as presented in Fig. 5. The referenced conventional polarizer transmits about 43% of an incident light. The difference in transmittance between DDLC polarizers with different dye concentrations is small at low voltages, and the transmittance begins to increase after 2 V and gradually reaches maximum

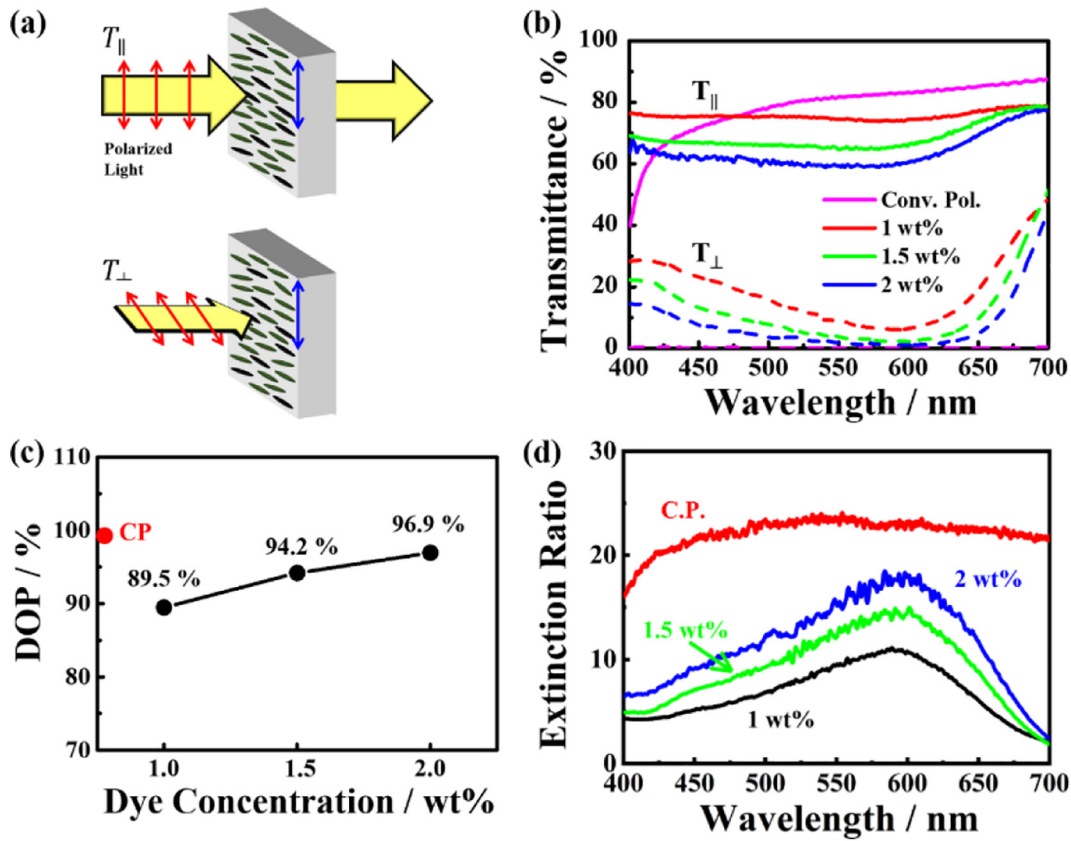


Fig. 4. (a) Schematics of measuring T_{\parallel} and T_{\perp} . The blue arrow indicates the transmission axis of the DDLC cells. The red arrows indicate the polarization direction of an incident light. (b) Measured wavelength-dependent T_{\parallel} (solid lines) and T_{\perp} (dashed lines). (c) Measured DOP at 550 nm. CP represents the conventional polarizer that is indicated by the red dot. (d) Measured ER of DDLC polarizers and conventional polarizer.

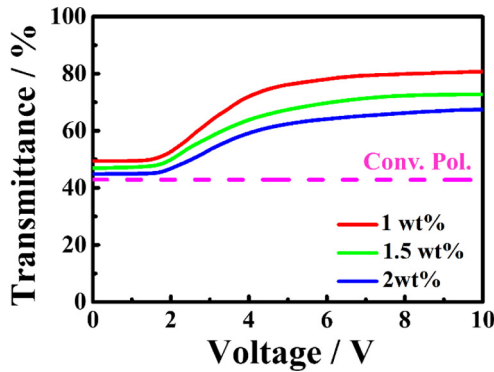


Fig. 5. Comparison of voltage-dependent transmittance of DDLC polarizers. The conventional polarizer was indicated as a dotted line.

transmission at 10 V, indicating the dye director follows reorientation of the LC director. In contrast to the conventional polarizer, a significant increase of transmittance was obtained for DDLC polarizers upon voltage supply because the dye director switched from planar to vertical alignment. Interestingly, the on-state transmittance can be further manipulated by controlling the dye concentration. The normalized voltage-dependent transmittance is shown in Fig. S4 and the whole cell images are shown in Fig. S5. The driving voltages are 5.8 V, 6.1 V, and 6.4 V for 1 wt%, 1.5 wt%, and 2 wt% DDLC polarizers, respectively.

We also analyzed the voltage-dependent electro-optic properties of the DDLC cells, to check their feasibility to serve as a switchable polarizer in the OLED display. For this purpose, we measured the

reflectance of the DDLC polarizer at R-mode with the QWP and the OLED panel. We employed a luminance meter in a folded geometry to measure the reflectance. The measurement scheme is illustrated in Fig. 6(a). An inbuilt lamp in the luminance meter irradiates directly on the sample and the subsequent reflected light is measured by rotating the detector in the path of the reflected luminance flux. Note that we measured only the specular reflectance of a specific angle (θ) by keeping both incident and reflected angles to 10° with respect to the cell's substrate. The reflectance data, as a function of wavelength, clearly confirms that the DDLC polarizer had a significant effect on a reflectance of 10° as depicted in Fig. 6(b). The reflectance with DDLC polarizers rapidly decreases with increasing dye concentration such that it is 17.85%, 10.66%, and 6.25% at 550 nm for 1 wt%, 1.5 wt%, and 2 wt% dye concentration, respectively. Since the reflectance of the conventional polarizer is 8.35%, the DDLC polarizer with 2 wt% was quite effective in suppressing the reflectance. As can be seen in Fig. 6(c), similar results were achieved for macroscopic images of the cells taken by a high-resolution camera. The images represent a manifestation of distinct reflectance with dye concentration. The 1 wt% sample shows more reflectance than that of the 2 wt% sample such that the shadow of the camera dimly appears in the 1 wt% sample whereas it vanished for 2 wt% sample. Thus, the proposed DDLC polarizer seems to be an efficient candidate to restrain the reflections of OLEDs.

To gain more insight into the reflectance, we measured the SCI and SCE reflectance by using an integrated sphere method also known as the Ulbricht Sphere method. Specular reflection refers to a viewing display at identical angles for both the incident and observer's angles; whereas diffuse reflection, also known as Lambertian reflection, refers to a viewing display at different incident and observer's angles. As the specular reflection can be eliminated by tilting the display device, the

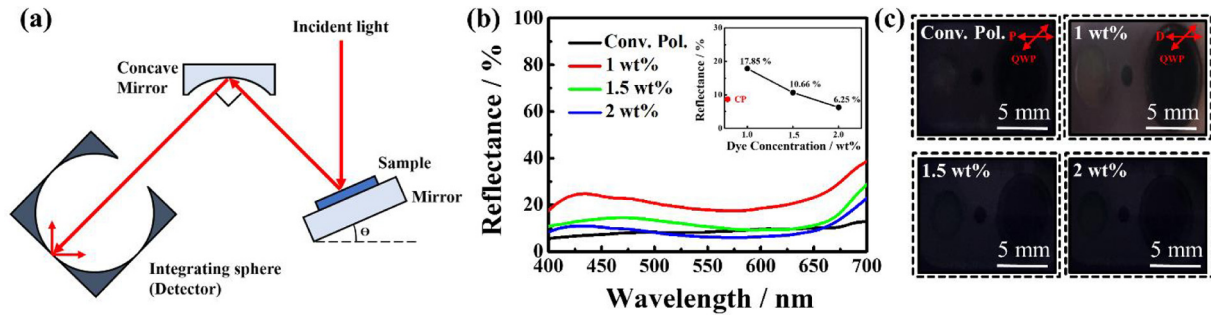


Fig. 6. (a) Schematic diagram of the reflectance measurements of prepared samples at P-mode. The θ represents the rotation angle of the sample. (b) Measured wavelength-dependent specular reflection of DDLC polarizer at 10° . Comparative results at 550 nm shown inset. (c) Corresponding macroscopic images. The p and D represent transmission axis of the conventional polarizer and the absorption axis of the DDLC polarizer.

actual human perception of the display is mainly associated with the diffuse reflection. The SCI and SCE reflectance measurements scheme are depicted in Fig. 7(a). Based on the instrument's geometry, the specular reflection is removed by opening a light trap, so that only diffuse reflection is measured. For SCI reflectance, both diffuse and specular reflections can be measured by closing the light trap. In order to make a quantitative comparison, we measured the SCI reflection with a sample angle from previous measurements ($10^\circ \pm 0.5^\circ$). The SCE reflection refers to the observer's angle that is not the specular angle. Both measurements were performed in an off-normal direction perpendicular to the display surface. Fig. 7(b) and (c) indicate the SCI reflection spectra and Fig. 7(d) and (e) represent the SCE reflection spectra. It is evident that a relatively higher reflectance was obtained when specular reflection was considered. More specifically, the reflectance of 1 wt% and 1.5 wt% DDLC polarizers was 22.43% and 10.49%, respectively, which is higher than the conventional polarizer (9.48%). Still, the reflectance of 2 wt% DDLC polarizer was approximately equal to the conventional polarizer. However, interestingly, a significant decrease in reflectance was obtained if we disregard the specular reflection. In the case of SCE, the reflectance measured at 550 nm was 1.79%, 5.79%, 1.75%, 1.4% for the conventional polarizer, and 1 wt%, 1.5 wt%, and 2 wt% for the

DDLC polarizers. Based on our study on reflectance, our device offers significantly less reflectance compared to the conventional polarizer.

Chromaticity properties of the reflected light were also measured to investigate whether or not SCI and SCE reflections possess any chromatic behavior. The specular reflection condition was measured at $0:10^\circ$ (zero degree incident angle and 10° observer's angle). The chromaticity diagrams of the SCI and SCE reflections of the DDLC polarizer were depicted in the CIE 1931 color space and 1976 color space as presented in Fig. 8. The u' and v' of the CIE 1976 were calculated by following Eq. [37];

$$u' = \frac{4x}{-2x + 12y + 3}, v' = \frac{9y}{-2x + 12y + 3} \quad (3)$$

where x and y are the chromaticity values of the specific color in CIE 1931 color space. The color coordinates of D65 illuminant were (0.31271, 0.32902) and (0.31382, 0.33100) for CIE 1931 and CIE 1976 color space, respectively. The (x, y) coordinates of CIE 1931 were converted to (u, v) coordinates of CIE 1976 color space using the above Eq. (3). By comparing both charts, one can notice that there is no chromaticity behavior of reflected light due to DDLC polarizer. The color difference (ΔC) was calculated from the equation [37],

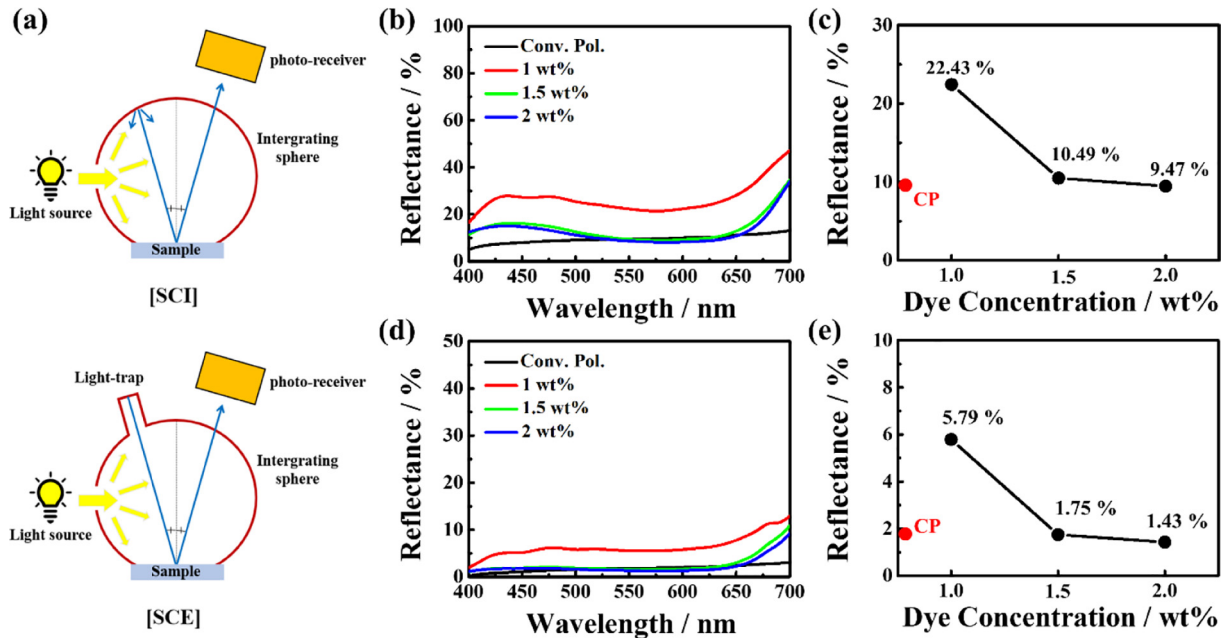


Fig. 7. (a) Schematic diagram of the SCI and SCE reflectance modes of the DDLC polarizer. Measured wavelength-dependent reflectance of (b) SCI mode and (d) SCE mode. Comparative results of, (c) SCI mode and, (e) SCE mode, calculated at 550 nm. CP represents a conventional polarizer.

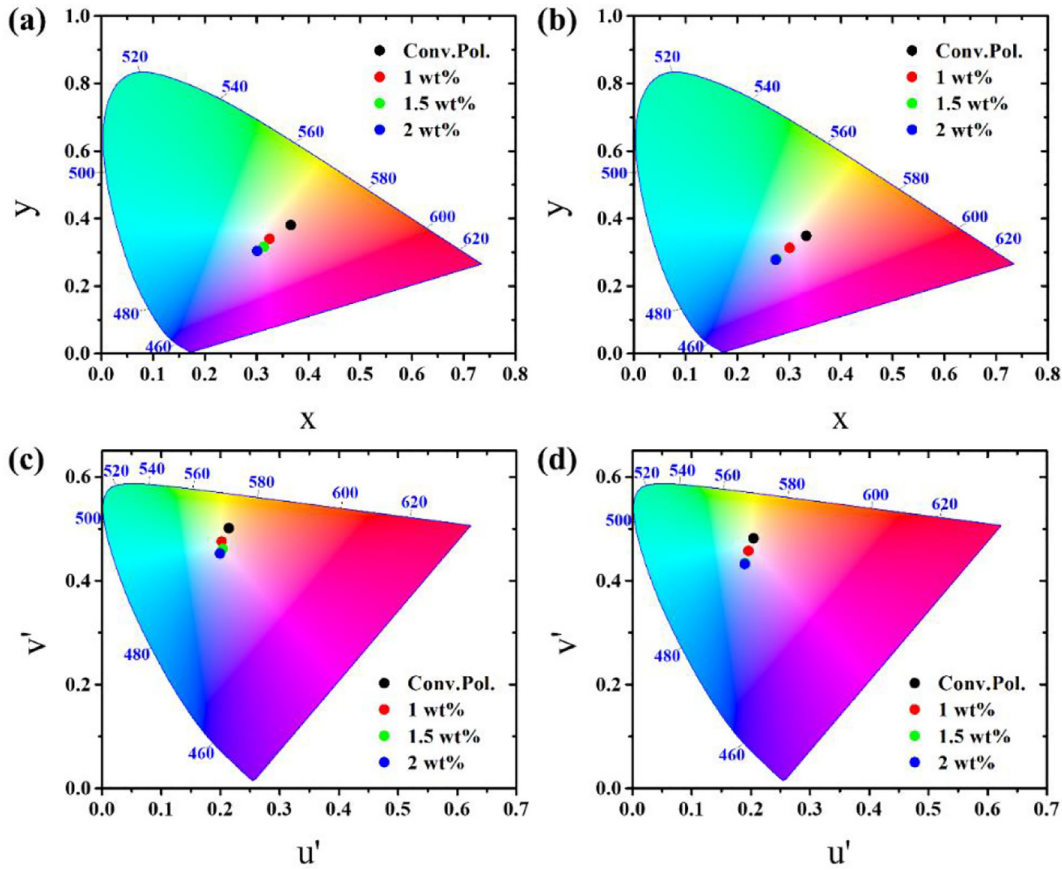


Fig. 8. Chromaticity diagram of the CIE 1931 color space at (a) SCE mode and (b) SCI mode. Chromaticity diagram of CIE 1976 color space at (c) SCE mode and (d) SCI mode.

$$\Delta C = \sqrt{(\Delta u')^2 + (\Delta v')^2} \tag{4}$$

where $\Delta u'$ and $\Delta v'$ are the difference in the coordinates. Interestingly, the conventional polarizer exhibits a slightly reddish nature. Unlike the reflectance intensity, the variation in the color coordinates within either SCI mode or SCE mode was not great, therefore we presume that all the DDLC polarizers do not show any viewing angle dependent chromaticity. For instance, the (0.20218, 0.47589) coordinates of the SCE reflection for 1 wt% DDLC polarizer shifted to (0.19565, 0.45775) in the CIE 1976 chart when we take the specular reflection into consideration. This indicates a relatively negligible chromaticity difference between

specular and diffuse reflections. The measured ΔC is smaller than ~ 0.03 for all the samples, which is not noticeable to human observation. Although a slight blue shift was noticed in SCI reflectance for 2 wt% dye sample, such little color difference exerts an imperceptible influence on the display quality. Ultimately, the data indicate that the specular reflection does not have much chromaticity effect.

In a final step, electro-optic switching characteristics of the DDLC polarizer were studied, which are a key property of our device. Fig. 9 (a) shows the wavelength-dependent transmission spectra of the DDLC polarizer in both P- and T-modes. In P-mode, the DDLC polarizer, having unidirectional ordering of dye molecules, absorbs the emitted light propagating along its long molecular axis, but transmits the

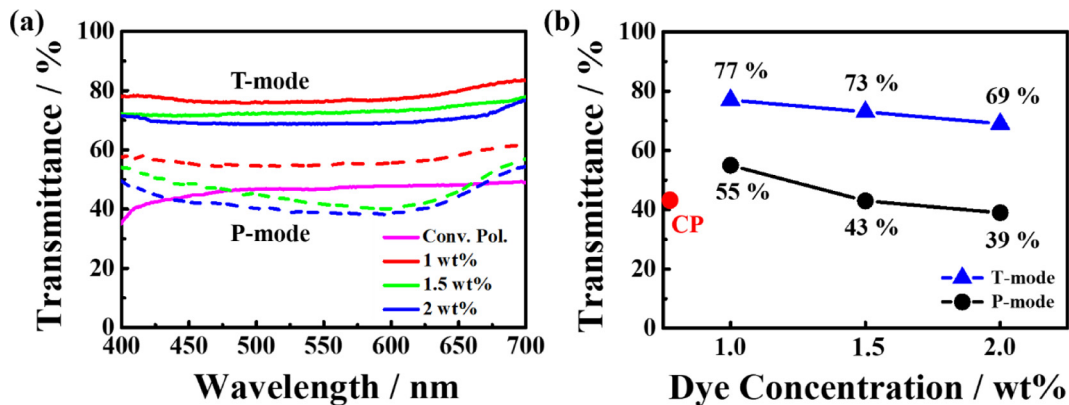


Fig. 9. (a) Measured wavelength-dependent transmittance of proposed switchable polarizer at P-mode (0 V, dotted lines) and T-modes (10 V, solid lines). (b) Relative transmittances of P- mode (black dots) and T-mode (blue triangles) are calculated at 550 nm.

emitted light propagating perpendicular to its long molecular axis. Each DDLC polarizer shows different levels of selective absorption that are governed by the dye concentration. Fig. 9(b) shows the quantitative comparison of transmittance between our proposed polarizers and a conventional polarizer calculated at 550 nm. The transmittance of the conventional polarizer was limited to 43% whereas the DDLC polarizer with 1 wt%, 1.5 wt%, and 2 wt% dye concentration exhibited 55%, 43%, and 39%, respectively. The transmittance decreases with increasing dye concentration, which is attributable to the possible increase in selective absorption of the emitted light with increasing dye concentration. As already described in the Fig. 1(c), the P-mode is associated with outdoor environments such as a sunny day or a bright office room. Our proposed DDLC polarizer can perform similarly to the conventional polarizer for outdoor applications. Very interesting results can be achieved when a voltage is supplied to the DDLC polarizer, i.e. the T-mode, which is associated with watching the display indoors with low ambient light conditions. Particularly, at the T-mode, the performance of the conventional polarizer is unaltered, but our DDLC polarizer shows significantly increased transmittance. It exhibits transmittance of 77%, 73%, and 70% for 1 wt%, 1.5 wt%, and 2 wt% dye concentrations, respectively. Only a quarter of the emitted light was sacrificed for the DDLC polarizer while more than half of the emitted light was wasted with the conventional polarizer. The transmittance increasing rate was 80%, 70%, and 61% for 1 wt%, 1.5 wt%, and 2 wt% dye concentrations, respectively. Such a large increase in transmittance undoubtedly originated from the switching of dye director from planar to vertical orientation. In addition, 1 wt% DDLC polarizer showed a relatively good wavelength dispersion whereas the other two polarizers of 1.5 wt% and 2 wt% samples showed a slight decrease in transmittance at the mid-visible spectra for P-mode. This can be significantly improved by adjusting the cyan-magenta-yellow mixing ratio. However, it almost vanished for T-mode due to the switching of the dye molecules into the non-absorbing direction. Overall, there is a delicate balance between the dye concentration, reflectance, and transmittance in perspective of image quality. For instance, with a higher dye concentration, the DDLC polarizer exhibits a low reflectance, but decreases the transmittance whereas it is opposite for low dye concentrations. However, the DDLC polarizer clearly has a greater advantage of achieving high transmittance compared to several conventional tunable and non-tunable polarizers [18,34,38,39]. It can refrain from the unnecessary supply of high current to the OLEDs to increase the display emission light, so that the lifetime of the OLEDs can be greatly improved. The disadvantage is that, unfortunately, an additional set of DDLC polarizers with driving circuits is required, which slightly increases the cost of the device.

5. Conclusions

We have tested an electrically switchable DDLC polarizer for an OLED display that can exhibit an optimal performance in both indoor and outdoor conditions. Under outdoor conditions with bright ambient light, it acts as a polarizer by selective absorption of ambient light and thereby reduces the reflectance. In contrast, when ambient light is dim, as for instance in many indoor environments, it can be switched into a low absorption state to allow most of the emitted light from the display to pass through. The proposed DDLC polarizer not only exhibits a 96% of DOP, but also eliminates both specular and diffuse reflections of ambient light. The DDLC polarizer increases optical efficiency up to 80% compared to the conventional polarizer under moderate ambient light conditions. The OLED can emit strong light without unnecessarily supplying additional power to the display panel. Ultimately, the proposed DDLC polarizer saves on power consumption and thereby improves the lifetime of the OLEDs which is a crucial technical barrier that needs to be overcome in current OLEDs.

Author statement

Y. Won and H.S. Shin prepared samples and performed majority of the experiments. M. Jo and Y.J. Lim performed chromaticity measurements. R. Manda analyzed the data and written the manuscript. The project was initiated and conceived by S.H. Lee.

Declaration of Competing Interest

The authors declare that they have no known competing financial interests or personal relationships that could have appeared to influence the work reported in this paper.

Acknowledgements

This research was supported by the Basic Science Research Program through the National Research Foundation of Korea (NRF) funded by the Ministry of Education (2016R1D1A1B01007189) and by the National Research Foundation of Korea (NRF) grant funded the Korea government (MSIT) (2019R1A5A80326).

Appendix A. Supplementary data

Supplementary data to this article can be found online at <https://doi.org/10.1016/j.molliq.2021.115922>.

References

- [1] C.D. Müller, A. Falcou, N. Reckefuss, M. Rojahn, V. Wiederhirn, P. Rudati, H. Frohne, O. Nuyken, H. Becker, K. Meerholz, Multi-colour organic light-emitting displays by solution processing, *Nature* 421 (6925) (2003) 829–833.
- [2] P.E. Burrows, G. Gu, V. Bulovic, Z. Shen, S.R. Forrest, M.E. Thompson, Achieving full-color organic light-emitting devices for lightweight, flat-panel displays, *IEEE Tran. Electron Dev.* 44 (8) (1997) 1188–1203.
- [3] B. Chen, B. Liu, J. Zeng, H. Nie, Y. Xiong, J. Zou, H. Ning, Z. Wang, Z. Zhao, B.Z. Tang, Efficient Bipolar Blue ALEgens for High-Performance Nondoped Blue OLEDs and Hybrid White OLEDs, *Adv. Funct. Mater.* 28 (40) (2018) 1803369.
- [4] G. He, M. Pfeiffer, K. Leo, M. Hofmann, J. Birstock, R. Pudlich, J. Salbeck, High-efficiency and low-voltage p-i-n electrophosphorescent organic light-emitting diodes with double-emission layers, *Appl. Phys. Lett.* 85 (17, 2004) 3911–3913.
- [5] B. Geffroy, P. Le Roy, C. Prat, Organic light-emitting diode (OLED) technology: materials, devices and display technologies, *Polym. Int.* 55 (6) (2006) 572–582.
- [6] C.W. Han, J.S. Park, H.S. Choi, T.S. Kim, Y.H. Shin, H.J. Shin, M.J. Lim, B.C. Kim, H.S. Kim, B.S. Kim, Y.H. Tak, Advanced technologies for UHD curved OLED TV, *J. Soc. Inf. Disp.* 22 (11, 2014) 552–563.
- [7] T.L. Chiu, K.H. Chuang, C.F. Lin, Y.H. Ho, J.H. Lee, C.C. Chao, M.K. Leung, D.H. Wan, C.Y. Li, H.L. Chen, Low reflection and photo-sensitive organic light-emitting device with perylene diimide and double-metal structure, *Thin Solid Films* 517 (13, 2009) 3712–3716.
- [8] L.S. Hung, J. Madathil, Reduction of ambient light reflection in organic light-emitting diodes, *Adv. Mater.* 13 (23, 2001) 1787–1790.
- [9] J.T. Lim, H. Lee, H. Cho, B.H. Kwon, N.S. Cho, B.K. Lee, J. Park, J. Kim, J.H. Han, J.H. Yang, B.G. Yu, Flexion bonding transfer of multilayered graphene as a top electrode in transparent organic light-emitting diodes, *Sci. Rep.* 5 (2015) 17748.
- [10] X. Wu, J. Liu, D. Wu, Y. Zhao, X. Shi, J. Wang, S. Huang, G. He, Highly conductive and uniform graphene oxide modified PEDOT: PSS electrodes for ITO-free organic light emitting diodes, *J. Mater. Chem. C* 2 (20, 2014) 4044–4050.
- [11] L. Hu, J. Li, J. Liu, G. Grüner, T. Marks, Flexible organic light-emitting diodes with transparent carbon nanotube electrodes: problems and solutions, *Nanotechnology* 21 (15, 2010) 155202.
- [12] Y.F. Liu, J. Feng, Y.G. Bi, D. Yin, H.B. Sun, Recent developments in flexible organic light-emitting devices, *Adv. Mater. Techn.* 4 (1) (2019) 1800371.
- [13] C.J. Yang, C.L. Lin, C.C. Wu, Y.H. Yeh, C.C. Cheng, Y.H. Kuo, T.H. Chen, High-contrast top-emitting organic light-emitting devices for active-matrix displays, *Appl. Phys. Lett.* 87 (14, 2005) 143507.
- [14] A.N. Krasnov, High-contrast organic light-emitting diodes on flexible substrates, *Appl. Phys. Lett.* 80 (20, 2002) 3853–3855.
- [15] X.D. Feng, R. Khangura, Z.H. Lu, Metal-organic-metal cathode for high-contrast organic light-emitting diodes, *Appl. Phys. Lett.* 85 (3) (2004) 497–499.
- [16] P.Y. Ang, P.A. Will, S. Lenk, A. Fischer, S. Reineke, Inside or outside: evaluation of the efficiency enhancement of OLEDs with applied external scattering layers, *Sci. Rep.* 9 (1) (2019) 1–10.
- [17] R. Singh, K.N. Unni, A. Solanki, Improving the contrast ratio of OLED displays: an analysis of various techniques, *Opt. Mater.* 34 (4) (2012) 716–723.

- [18] Y. Takahashi, Y. Furuki, S. Yoshida, T. Otani, M. Muto, Y. Suga, Y. Ito, 29.1: A New Achromatic Quarter-Wave Film Using Liquid-Crystal Materials for Anti-Reflection of OLEDs, SID Symposium Digest Tech. Pap. 45 (1) (2014) 381–384.
- [19] K. Osato, T. Kobayashi, P-140: novel $\frac{1}{4}$ -wave plate film for OLED panels, SID Symposium Digest Tech. Pap. 46 (1) (2015) 1687–1690.
- [20] S.W. Oh, S.H. Kim, J.M. Baek, T.H. Yoon, Design of an achromatic wide-view circular polarizer using normal dispersion films, J. Information Display 20 (1) (2019) 25–30.
- [21] H.J. Noh, C.M. Ahn, T.W. Ko, C.S. Lim, S.H. Choi, Y.H. Shin, J.M. Kim, M.C. Jun, C.H. Oh, I.B. Kang, 71-2: new Technology of Improving Blackness for OLED TV, SID Symposium Digest Tech. Pap. 48 (1) (2017) 1038–1040.
- [22] Y.J. Choi, Y. Lee, G. Bang, J. Jeong, N. Kim, J.H. Lee, K.U. Jeong, Lattice-work nanostructure by chemical function transfer and molecular shape amplification of programmed reactive mesogens, Adv. Funct. Mater. 29 (44) (2019) 1905214.
- [23] Z. Qin, K.C. Lee, Y.W. Yeh, Y.P. Huang, H.P. Shieh, 31-3: suppression of ambient-light reflection in OLED display by using a micro-lens Array and cruciform black matrices, SID Symposium Digest Tech. Pap. 47 (1) (2016) 397–400.
- [24] P. Fournet, J.N. Coleman, B. Lahr, A. Drury, W.J. Blau, D.F. O'Brien, H.H. Hörhold, Enhanced brightness in organic light-emitting diodes using a carbon nanotube composite as an electron-transport layer, J. Appl. Phys. 90 (2) (2001) 969–975.
- [25] D. Zhang, K. Ryu, X. Liu, E. Polikarpov, J. Ly, M.E. Tompson, C. Zhou, Transparent, conductive, and flexible carbon nanotube films and their application in organic light-emitting diodes, Nano Lett. 6 (9) (2006) 1880–1886.
- [26] Y.J. Bae, H.J. Yang, S.H. Shin, K.U. Jeong, M.H. Lee, A novel thin film polarizer from photocurable non-aqueous lyotropic chromonic liquid crystal solutions, J. Mater. Chem. 21 (7) (2011) 2074–2077.
- [27] Y.V. Bludov, M.I. Vasilevskiy, N.M. Peres, Tunable graphene-based polarizer, J. Appl. Phys. 112 (8) (2012), 084320.
- [28] H.G. Lee, C.S. Lee, S.G. Lee, Y.J. Heo, Y.J. Lim, S.H. Lee, P-106: guest-host liquid crystal devices utilizing dichroic dye and its application, SID Symposium Digest Tech. Pap. 50 (1) (2019) 1652–1655.
- [29] K. Kim, Y.J. Lim, L.V. Doan, G.D. Lee, S.H. Lee, Antireflective film design to improve the optical efficiency of organic light-emitting diode displays, Korean J. Opt. Photonics 29 (6) (2018) 262–267.
- [30] Y. Choi, S.W. Oh, T.H. Choi, B.H. Yu, T.H. Yoon, Formation of polymer structure by thermally-induced phase separation for a dye-doped liquid crystal light shutter, Dyes Pigments 163 (2019) 749–753.
- [31] V.K. Baliyan, K.U. Jeong, S.W. Kang, Dichroic-dye-doped short pitch cholesteric liquid crystals for the application of electrically switchable smart windows, Dyes Pigments 166 (2019) 403–409.
- [32] S.M. Ji, S.W. Oh, Y.S. Jo, S.M. Nam, S.H. Kim, J.W. Huh, E. Lim, J. Kim, T.H. Yoon, Optimization of dye mixing for achromatic transmittance control with a dye-doped cholesteric liquid crystal cell, Dyes Pigments 160 (2019) 172–176.
- [33] M.T. Sims, L.C. Abbott, S.J. Cowling, J.W. Goodby, J.N. Moore, Dyes in liquid crystals: experimental and computational studies of a guest-host system based on a combined DFT and MD approach, Chem. Eur. J. 21 (28, 2015) 10123–10130.
- [34] H.S. Shin, R. Manda, T.H. Kim, J.G. Park, Y.J. Lim, B.K. Kim, Y.H. Lee, S.H. Lee, Multi-layered carbon nanotube UV polariser for photo-alignment of liquid crystals, Liq. Cryst. 47 (11, 2020) 1604–1611.
- [35] Y. Zhang, Q. Liu, H. Mundoor, Y. Yuan, I.I. Smalyukh, Metal nanoparticle dispersion, alignment, and assembly in nematic liquid crystals for applications in switchable plasmonic color filters and E-polarizers, ACS Nano 9 (3) (2015) 3097–3108.
- [36] G. Myhre, A. Sayyad, S. Pau, Patterned color liquid crystal polymer polarizers, Opt. Express 18 (26, 2010) 27777–27786.
- [37] A.R. Robertson, The CIE 1976 color-difference formulae, Color. Res. Appl. 2 (1) (1977) 7–11.
- [38] S. Shoji, H. Suzuki, R.P. Zaccaria, Z. Sekkat, S. Kawata, Optical polarizer made of uniaxially aligned short single-wall carbon nanotubes embedded in a polymer film, Phys. Rev. B 77 (15) (2008) 153407.
- [39] H.J. Jin, K.H. Kim, H. Jin, J. Chang Kim, T.H. Yoon, Dye-doped liquid crystal device switchable between reflective and transmissive modes, J. Information Display 12 (1) (2011) 17–21.